Chapter 3: Tri-uniform Bond Stress Distribution

This chapter is going to present a proposed tri-bond stress distribution, a methodology to verify the proposed model, and a parametric investigation based on the proposed model.

3.1 Tri-uniform bond stress model

The bi-uniform bond stress distribution model (Fig 2.13) along lap splice was proposed by Sezen and Moehle (2003) to calculated entire slip of a bar anchored into a footing. It was also applied to estimate an anchorage bar strength and lap splice strength [Matrin (2007)]. However, the bond stress value in two zones, plastic and elastic, were assumed by Sezen and Moehle (2003) or back-calculated from design codes [ACI318 (2005)], by Matrin (2007); Therefore, bond stress and slip are in no relation, which is quite irrational since bond stress is experimentally depended on a slip. Moreover, It is impossible to apply an experimentally proposed bond-slip relationship model to the bi-uniform bond stress distribution model to determine bond stress in either lap splice unconfined and confined by FRP, because bond stress and slip in any bond-slip model cannot be applied simultaneously, calculated slip from bi-uniform bond stress distribution model is never equal to the corresponding slip in bond-slip model, it is often larger than that in bond slip model. An idea of tri-uniform bond stress distribution model consists of three zones presented in this section can solve these issues.

Fig 3.1 shows a column with longitudinal bars spliced with the starter bars at the base of the column. When the column is subjected to an applied load, a crack occurs at the interface between column base and footing (point O). Consider an outermost bar on the tension side, the developed bar stress f_s at the starting point of the lap splice zone (point O) must be in equilibrium with bond stresses on the bar surface along the lap length. The bond stress distribution along the lap splice length L_s depends on many factors such as the pull-out force $A_s f_s$, the length of the lap splice L_s, the confinement condition, and so on. An example of bond stress distribution before lap splice failure is shown in Fig 3.1 (1), in which u_y and u_e, are bond stresses acting on yielding zone and elastic zone, respectively.

At the critical state of splitting failure, the bond stress distribution along the lap splice length is assumed to follow the tri-uniform bond model as shown in Fig 3.1 (2a). In the model, the lap splice length is divided into three zones; namely, yielding zone (OA), post-splitting zone (AB) and splitting zone (BC), with bond stresses on each zone denoted by u_y, u_r and u_{sp} respectively. The lengths of yielding zone, post-splitting zone, and splitting zone are L_y, L_r and L_{sp} respectively. The sum of these lengths must be equal to the lap splice length L_s.

$$L_s = L_y + L_r + L_{sp} \tag{3.1}$$

The tri-uniform bond model is different from the model (Fig 2.13) proposed by Sezen and Moehle (2003) for predicting the slip of bars anchored into footing in that the bond stress in the elastic zone (AC) is assumed to be composed of splitting zone (BC) and post-splitting zone (AB) while Sezen and Moehle assumed a constant bond stress equal to two times bond strength in the yield zone. Fig 3.1 (2b, 2c) shows a tri-linear distribution of stress and strain in reinforcing bars. The steel stress and strain are zero at the end of lap

splice (C) and increases to (f_{sp},ε_{sp}) at point B. In the post-splitting zone (AB), bar stress and strain are increased from f_{sp} and ε_{sp} at point B to yield point f_y and ε_y at point A. At point A which separates the bar into elastic and yielding zones, the strain exhibits a discontinuous jump from ε_y to ε_{sh}, which is the strain at the onset of strain hardening. In the next section, the bond stress models are described for each zone. By combining the equilibrium equations, steel strain-slip relation and bond slip models, the steel stress – slip relation of the lap splice can be derived.

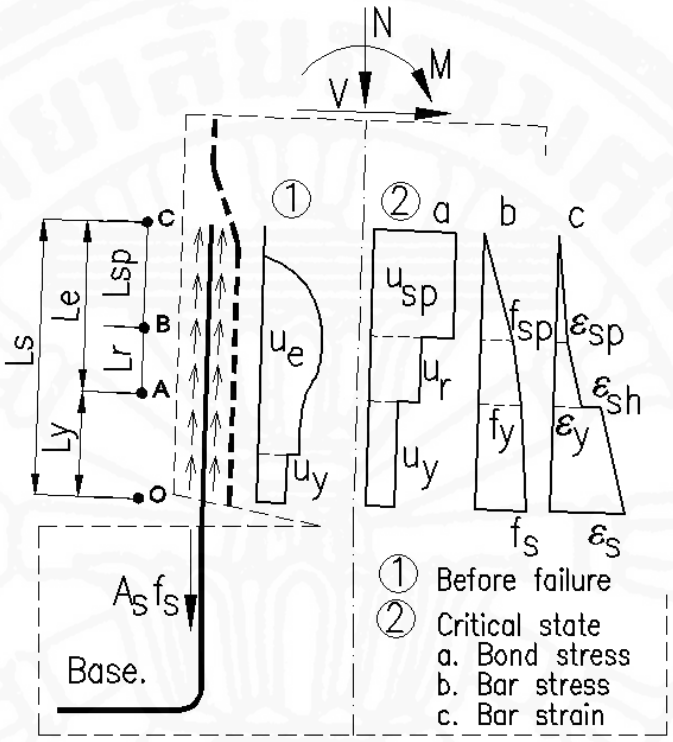

Fig 3.1: Tri-uniform bond stress model

3.2 Bond stress – slip model of lap splice confined by FRP

In the splitting zone of the tri-uniform bond model, the uniform bond stress (u_{sp}) can be obtained from the bond stress –slip model of lap splice confined by FRP. Wrapping FRP around lap splice zone induces additional lateral stress, thereby increasing the bond stress of the spliced bar. In order to simulate the bond-slip behavior of spliced bars strengthened by FRP, a bond-slip model (Fig 3.2) proposed by Harajli (2006) is adopted in this paper. In this model, the peak bond stress u_{sp} and the corresponding slip s_{sp} at bond splitting failure are expressed by Eq. (3.2) and Eq. (3.3) respectively. It is noted that in the Eq. (3.2), a proposed factor of 1.20 was added to original expression in order to convert a peak value of local bond strength to splitting uniform bond strength. In the equations, u_m is the maximum bond stress at pullout mode of bond failure given as $u_m = 2.57\sqrt{f_c'}$; n_f and t_f are the number and the thickness of FRP sheets, respectively. The bond stress u_p on the decreasing curve is calculated using Eq. (3.4). The factor α_f, that represents the method of wrapping, is expressed by Eq. (3.5), in which N_f is the number of FRP strips with equal width b_f and for full wrapping, $\alpha_f = 1$.

$$u_{sp} = \frac{0.75\sqrt{f_c'}}{1.20}\left(\frac{c + 56\frac{E_f \alpha_f n_f t_f}{E_s n_s}}{d_b}\right)^{2/3} \leq u_m = 2.57\sqrt{f_c'} \tag{3.2}$$

$$s_{sp} = s_1 e^{3.3\, ln\left(\frac{u_{sp}}{u_m}\right)} + s_o\, ln\left(\frac{u_m}{u_{sp}}\right) \tag{3.3}$$

$$u_p = u_{sp}\left(0.5 + 46\frac{E_f \alpha_f n_f t_f}{E_s c n_s}\right) \leq u_{sp} \tag{3.4}$$

$$\alpha_f = \frac{N_f b_f}{L_s} \tag{3.5}$$

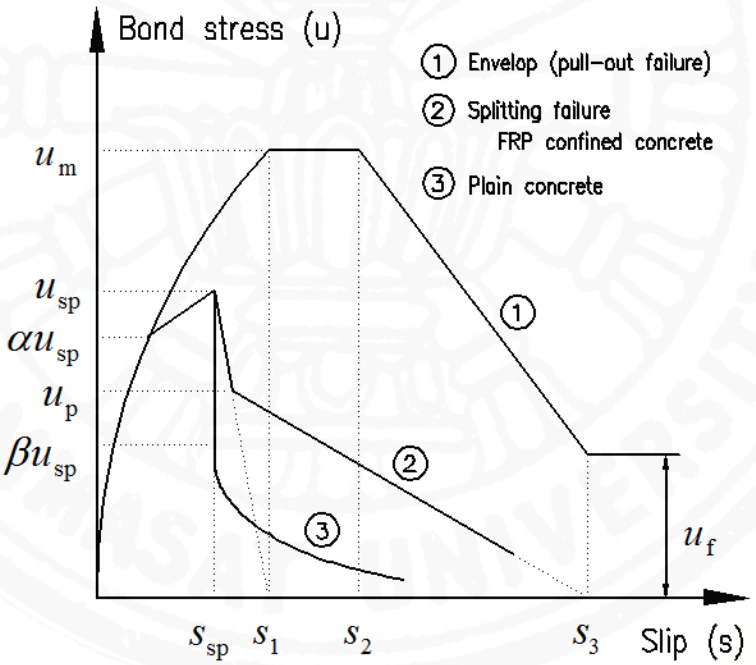

Fig 3.2: Bond stress–slip model by Harajli (2006)

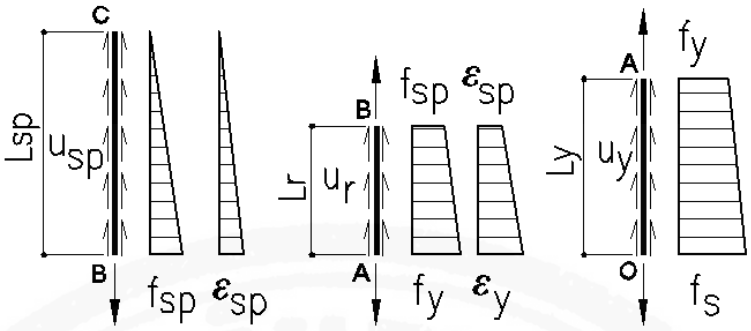

a)Splitting zone b)Post-splitting zone c)Yielding zone

Fig 3.3: Free body diagram

Other notations in the above equations are as follows: E_f, E_s are the modulus of elasticity of FRP sheets and transverse steels respectively; n_s is number of lap splices in tension; c is the concrete cover depth, s_0, s_1 and s_2 are local slip parameters that are computed from the clear distance between ribs on the reinforcing bar c_0. The details of the model can be found in Harajli (2006)'s paper.

3.3 Steel stress-strain model

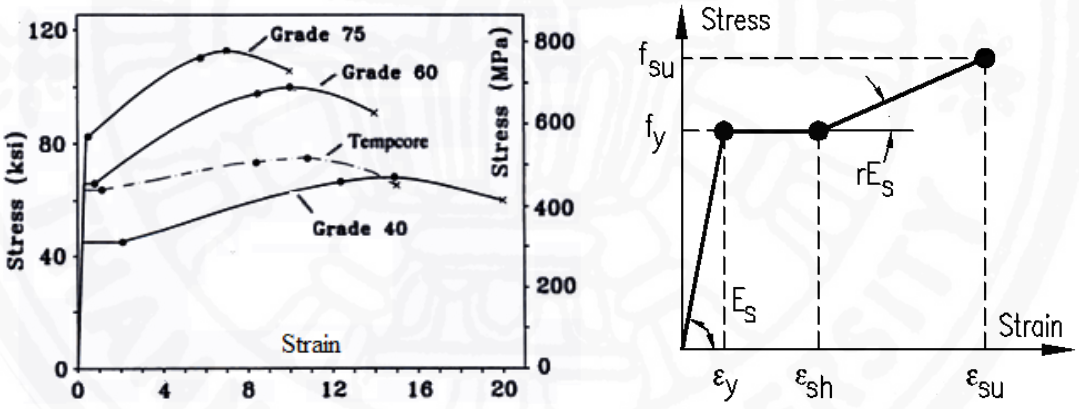

a) b)

Fig 3.4: Uniaxial stress-strain [Park and Paulay (1975)].
a) Actual relationship
b) Idealized model

A tri-linear stress-strain model is adopted from Park and Paulay (1975). Fig 3.4(a) shows the experimental stress-strain curve for steel grade 40, 60 and 75. Fig 3.4 (b) shows the idealized tri-linear stress–strain model. The steel stress-strain relationship is described by equations (3.6) to (3.8) .

$$f_s = E_s\varepsilon_s \qquad \text{If } \varepsilon_s \le \varepsilon_y = f_y/E_s \tag{3.6}$$

$$f_s = f_y \qquad \text{If } \varepsilon_y < \varepsilon_s < \varepsilon_{sh} \tag{3.7}$$

$$f_s = f_y + rE_s(\varepsilon_s - \varepsilon_{sh}) \qquad \text{If } \varepsilon_{sh} \le \varepsilon_s \le \varepsilon_{su} \tag{3.8}$$

Where f_s; ε_s are the bar stress and strain, E_s is the Young modulus of steel, f_y; ε_y are the yield stress and yield strain of steel, ε_{sh} is the bar strain at start of strain hardening, and ε_{su} is the strain at steel fracture. In order to apply the idealized stress-strain model to analyzing, the stress at hardening strain f_{sh}.is added and different from yielding stress f_y for example: $f_{sh} = 1.01 f_y$; by do so, a segment in the model from yielding point to hardening point is determined in analytical program.

3.4 Equilibrium and strain-slip condition

Fig 3.3 illustrates the free-body diagrams of the splitting zone (Fig 3.3a), post-splitting zone (Fig 3.3b) and yielding zone (Fig 3.3c). In each zone, the equilibrium equation between bond stress and bar stress can be derived. The slip of the bar can be calculated by integrating the strain along the lap splice. The steel stress (f_s) and the slip (s) can thus be calculated by

$$f_s = \left(u_{sp}\, L_{sp} + u_r\, L_r + u_y\, L_y\right) P \tag{3.9}$$

$$s = \int \varepsilon_s\, dx + s_0 \tag{3.10}$$

Where, P is the bar perimeter; ε_s is the strain in steel bar; and s_0 is the free slip (if any) at the end of lap splice. If the lengths of the three zones are known, it is possible to calculate the steel stress versus slip relation. In the next section, the equilibrium condition and the steel strain-slip relation will be described for each zone.

3.4.1 Splitting zone

A free body diagram and distribution of bar stress and bar strain along this zone are shown in Fig 3.3a. The bond and bar stresses have to satisfy Eq. (3.11).

$$u_{sp}(\pi d_b) L_{sp} = f_{sp} \frac{\pi d_b^2}{4} \qquad \text{Therefore: } f_{sp} = \frac{4 u_{sp} L_{sp}}{d_b} \tag{3.11}$$

To ensure that the splitting bond stress reaches the bond strength, the slip at point B has to attain the value of s_{sp} as shown in Eq. (3.12).

$$s_B = \frac{\varepsilon_{sp} L_{sp}}{2} = s_{sp} \qquad \text{Therefore:} \qquad \frac{f_{sp} L_{sp}}{2 E_s} = s_{sp} \tag{3.12}$$

By substituting Eq. (3.11) into Eq. (3.12), the expression for calculating the length of splitting zone can be derived in Eq. (3.13) in which the splitting bond strength $u_{sp}$and the corresponding slip s_{sp} are given in Eq. (3.2) and Eq. (3.3) respectively.

$$L_{sp} = \sqrt{\frac{E_s d_b}{2} \frac{s_{sp}}{u_{sp}}} \tag{3.13}$$

3.4.2 Post splitting zone

Fig 3.3b shows the free body diagram and distribution of bar stress and strain along this zone. The bond and bar stresses have to satisfy the equilibrium expressed by Eq. (3.14).

$$u_r(\pi d_b)L_r = \left(f_y - f_{sp}\right)\frac{\pi d_b^2}{4} \quad \text{Therefore:} \qquad L_r = (f_y - f_{sp})\frac{d_b}{4u_r} \tag{3.14}$$

To compute the length of the post splitting zone (L_r), the uniform bond stress u_r has to be determined. Fig 3.5 shows how to calculate the bond stress on post-splitting zone based on the bond stress - slip model of lap splice strengthened by FRP wrapping. In the figure, the relationship between post splitting bond stress (u_r) and corresponding slip is represented by a polyline m-n-q. An example of calculating bond stress u_r for a specified slip s_A is illustrated in Fig 3.5.

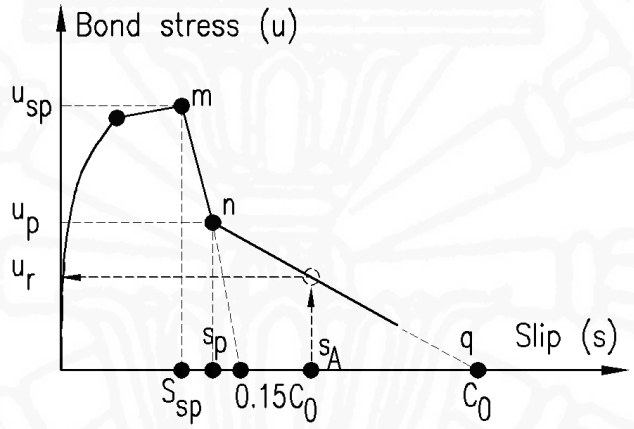

Fig 3.5: Calculation of bond stress for a specific slip s_A

In Fig 3.5, c_0 is the distance between the ribs of a reinforcing bar. Depending on the slip at point A, the bond stress can be computed following the line m-n-q. Expressions (3.15a) and (3.15b) are equations of these lines. In these equations, s_p is the slip at bond stress u_p which is calculated by Eq. (3.4).

$$u_r = \frac{0.15c_0 - s_A}{0.15c_0 - s_{sp}}u_{sp} \qquad \text{If } s_A \le s_p \tag{3.15a}$$

$$u_r = \frac{c_0 - s_A}{c_0 - s_p}u_p \qquad \text{If } s_A \ge s_p \tag{3.15b}$$

$$s_p = s_{sp} + \left(1 - \frac{u_p}{u_{sp}}\right)(0.15c_0 - s_{sp}) \tag{3.16}$$

The slip at point A is calculated from bar strain distribution along this zone as follows.

$$s_A = s_{sp} + \frac{(\varepsilon_{sp} + \varepsilon_y)L_r}{2} \tag{3.17}$$

Substituting u_r and s_A from Eqs. (3.15a, b) and (3.17) into Eq. (3.14), and rearranging the terms, Eqs. (3.18a) and (3.18b) for determining the length L_r of the post splitting zone are derived. It is noted that the length of post splitting zone will be determined from Eq. (3.18a) if the length is less than L_n given in Eq. (3.19), otherwise it will be obtained from Eq. (3.18b).

$$\frac{\varepsilon_{sp} + \varepsilon_y}{2(0.15c_0 - s_{sp})}L_r^2 - L_r + \frac{(f_y - f_{sp})d_b}{4u_{sp}} = 0 \tag{3.18a}$$

$$\frac{\varepsilon_{sp} + \varepsilon_y}{2(c_0 - s_p)}L_r^2 - \frac{c_0 - s_{sp}}{c_0 - s_p}L_r + \frac{(f_y - f_{sp})d_b}{4u_p} = 0 \tag{3.18b}$$

$$L_n = \frac{2(s_p - s_{sp})}{\varepsilon_{sp} + \varepsilon_y} \tag{3.19}$$

3.4.3 Yielding zone

A free body diagram and distribution of bar stress and bar strain along this zone are shown in Fig 3.3c. The bond and bar stresses have to satisfy equilibrium expressed by Eq. (3.20). The entire lap splice slip sO can be obtained from Eq. (3.21).

$$u_y(\pi d_b)L_y = (f_s - f_y)\frac{\pi d_b^2}{4} \leftrightarrow L_y = (f_s - f_y)\frac{d_b}{4u_y} \tag{3.20}$$

$$s_O = s_A + \frac{(\varepsilon_{sh} + \varepsilon_s)L_y}{2} \tag{3.21}$$

To compute the length of yielding zone, the bond stress u_y has to be determined. However, there is no model of bond and slip relationship proposed for the yielding bars. In an effort to calculate the bond slip of bars anchored into the basement, Sezen and Moehle (2003) used a bi-uniform bond stress model to simulate the slip behavior of bars in yielding range. They assumed a constant bond stress of $0.5\sqrt{f_c'}$ along the yielded portion of the bar. An experimental program on pull-out test was conducted to make an assessment on bond characteristics in post-yield range of deformed bar by Shima, Chou et al. (1987). In the test, the embedment length was set to $50d_b$ ($d_b = 19mm$) which was so sufficiently long that no free end slip occurred even if the bar reached yielding during pull-out. Fig 3.6 show the experimental results of three types of steel with different nominal yield strengths 300, 500 and 700 MPa, referred to as SD30, SD50 and SD70 respectively. As observed from the Fig 3.6, it is found that the bond stress acting along the yielding zone tends to be uniformly distributed and is equal to $u_y = 0.25{f_c'}^{2/3}$.

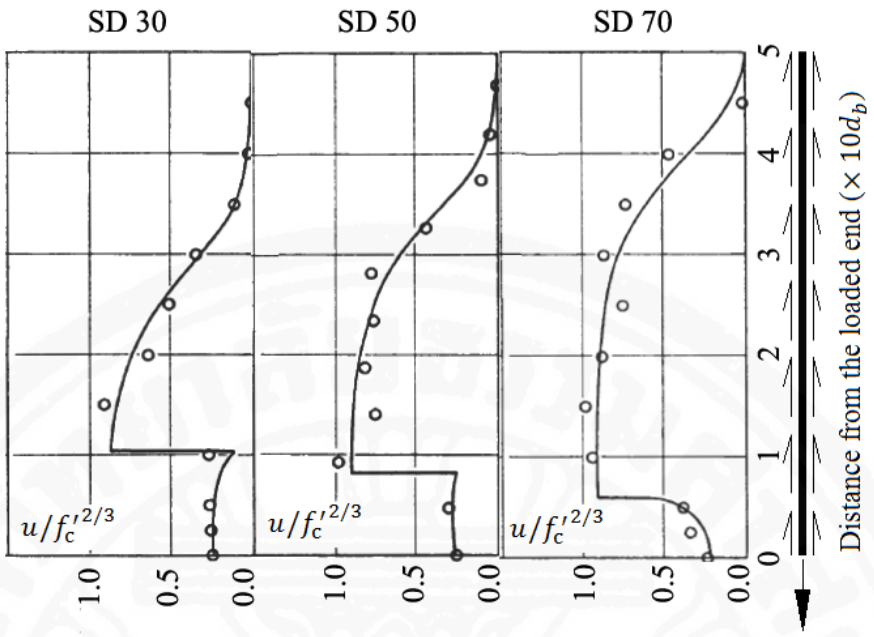

Fig 3.6: Experimental result by Shima, Chou et al. (1987)

From these researches, the bond stress in yielding zone is assumed to be $u_y = 0.25{f_c'}^{2/3}$, based on Shima, Chou et al. (1987) experimental data. Since wrapping FRP around column bar lap splice increases the compressive strength of concrete, the confined compressive strength of concrete f'_{cc} is used to calculate the bond stress in the yielding zone.

$$u_y = 0.25{f'_{cc}}^{2/3} \tag{3.22}$$

Substituting Eq. (3.22) into Eq. (3.20), we obtain Eq. (3.23) for calculating the length of yielding zone.

$$L_y = (f_s - f_y)\frac{d_b}{{f'_{cc}}^{2/3}} \tag{3.23}$$

3.5 Explicit equation for lap splice strength (both elastic and post-yield range)

For a reinforced concrete column with lap splice zone confined by FRP, and with known parameters including the length of lap splice, the concrete cover depth of reinforcing bar, the properties of concrete and steel materials, the characteristics of FRP sheets, and others, it is possible to determine the length of splitting zone, post-splitting zone and yielding zone as functions of the number and thickness of FRP sheets $n_f t_f$ by using Eqs. (3.13), (3.18a,b) and (3.23) respectively. Then the steel stress f_s and corresponding slip s can be computed by Eqs. (3.9) and (3.10), respectively. Thus, a steel stress – slip relation can be derived and the lap splice strength is determined as the maximum stress from the calculated relation.

However, rather than constructing the entire steel stress-slip relation, it is also possible to derive explicit equations for the lap splice strength. For known parameters as mentioned above, the post-yield strength of lap splice $[f_s]$ can be calculated from Eq. (3.24) which is obtained by imposing the condition of Eq. (3.1) that the total length of the three zones must

be equal to the length of lap splice L_s. It is noted that in Eq. (3.24), the variable L_r can be obtained by solving the Eq. (3.18a) or Eq. (3.18b).

$$[f_s] = f_y + \left(L_s - L_r - \sqrt{\frac{E_s d_b}{2} \frac{s_{sp}}{u_{sp}}} \right) \frac{f_{cc}'^{2/3}}{d_b} \tag{3.24}$$

In case that the bar stress at point B reaches the yield stress ($f_{sp} = f_y$), or the lap splice length is not sufficient to develop the post-splitting zone, the bond stress distribution along the splice length will consist of two zones, that is, yielding zone and splitting zone. In this case, a free slip s_0 must exist at the end point (C) of lap splice length to compensate the slip at point B in order to develop bond splitting strength u_{sp} [Alsiwat and Saatcioglu (1992)]. Fig 3.7 shows the bond and bar stress distribution along lap splice length. The lap splice strength can be estimated by Eq. (3.25) and finally by Eq. (3.26), in which L_{sp} is the length of splitting zone which can be computed from Eq. (3.11) by replacing the terms f_{sp} with yield stress f_y.

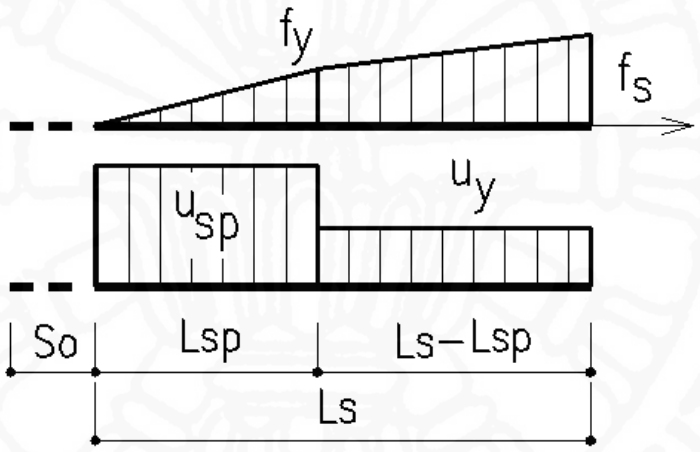

Fig 3.7: Free slip at the end of lap splice length

$$[f_s] = \frac{4}{d_b}(u_y L_s + (u_{sp} - u_y) L_{sp}) \tag{3.25}$$

$$[f_s] = \frac{f_{cc}'^{2/3}}{d_b} \left(L_s + \frac{f_y d_b}{f_{cc}'^{2/3}} - 0.25 \frac{f_y d_b}{u_{sp}} \right) \tag{3.26}$$

Fig 3.8 shows the flow chart of computational procedure to predict the post-yield strength of lap splice confined by FRP.

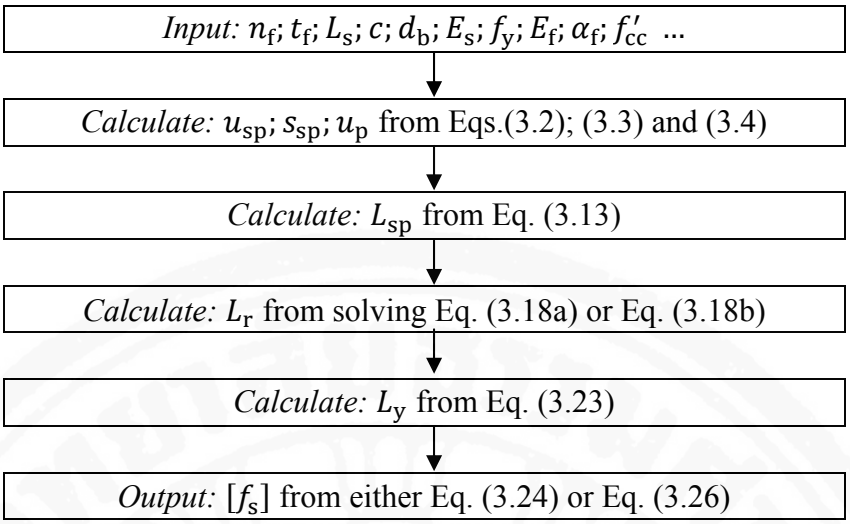

Fig 3.8: Calculation steps for lap splice strength

It is noted that the discussion above concerns about the post-yield strength of lap splice. However, the lap splice strength in the elastic range of reinforcing bar can also be computed by applying one or two parts of the tri-uniform bond stress model. There are two circumstances regarding the strength of lap splice in the elastic range. The first circumstance occurs when the lap splice length is sufficient so that bond stress can be developed to the splitting strength ($L_s \geq L_{sp}$). In this case, the bond stress distribution along the lap splice length will consist of two zones, that is, splitting zone and post-splitting zone. The elastic strength of lap splice is given by Eq. (3.18c) if $L_s - L_{sp} < L_n$, or Eq. (3.18d) if $L_s - L_{sp} \geq L_n$. Eqs. (3.18c) and (3.18d) are derived from Eqs. (3.18a) and (3.18b) by replacing f_y with $[f_s]$. The second situation occurs when the lap splice length is insufficient for the bond stress to reach the splitting strength ($L_s < L_{sp}$). In this case, there is a free slip at the end of lap splice (point C in Fig 3.1). There is only the splitting zone in the bond stress distribution and the elastic strength of the lap splice can be calculated by Eq. (3.27).

$$[f_s] = f_{sp} + \frac{4(L_s - L_{sp})u_{sp}}{d_b}\left(1 - \frac{(\varepsilon_{sp} + \varepsilon_y)(L_s - L_{sp})}{2(0.15c_0 - s_{sp})}\right) \tag{3.18c}$$

$$[f_s] = f_{sp} + \frac{4(L_s - L_{sp})u_p}{d_b}\left(\frac{c_0 - s_{sp}}{c_0 - s_p} - \frac{(\varepsilon_{sp} + \varepsilon_y)(L_s - L_{sp})}{2(c_0 - s_p)}\right) \tag{3.18d}$$

$$[f_s] = \frac{4u_{sp}L_s}{d_b} \tag{3.27}$$

3.6 Calculation procedure for required FRP thickness to reach a desired stress

In the previous section, the equations for predicting the lap splice strength have been derived in both elastic and post-yield ranges of steel bars at the splitting failure. For design purpose, it may be useful to derive equations for computing the required FRP thickness or the amount of FRP sheet for a given desired lap splice strength (or steel stress). Basically, the equations for the required FRP thickness express the inverse relation of the equations

for predicting the strength. However, as observed in Eq. (3.24), the right hand-side of the equation contains a complicated expression for $n_f t_f$, thus, it is very difficult to convert Eq. (3.24) into the form that explicitly calculates the thickness of FRP as a function of the lap splice length. Alternatively, the required thickness or the number of FRP sheets can be determined by applying the calculation produce as shown in Fig 3.9 based on trial and error procedure. The key mechanism of the proposed calculation procedure is to adjust the FRP thickness $n_f t_f$ so that the condition given in Eq. (3.1) that the sum of lengths of the three zones is equal to the lap splice length is satisfied.

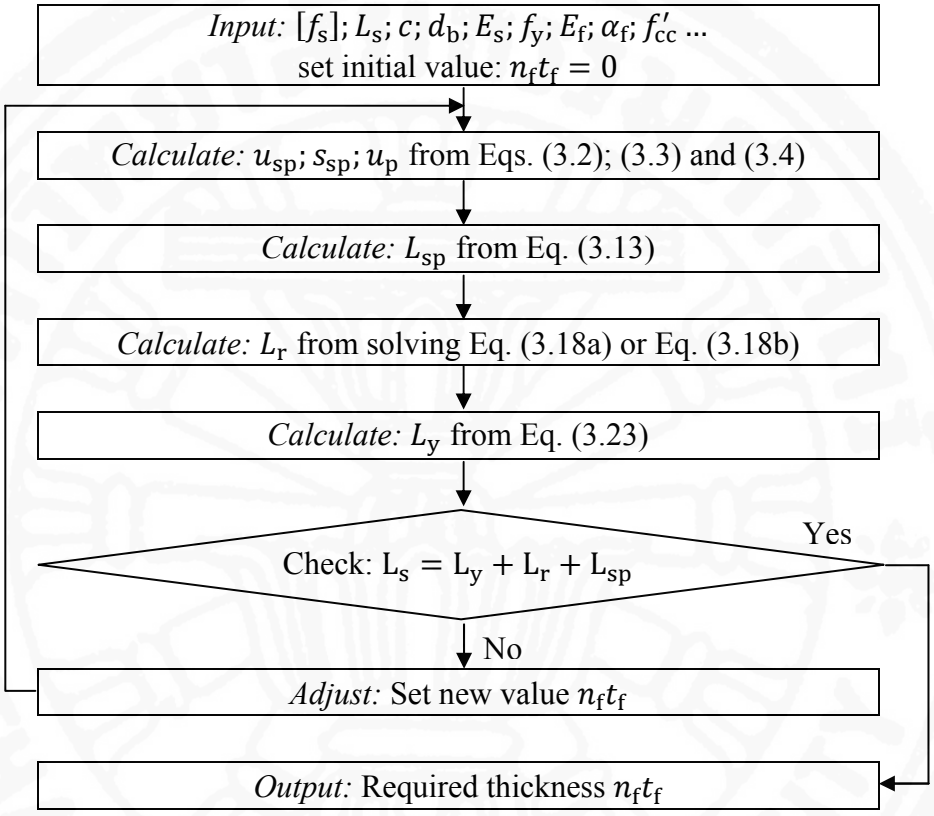

Fig 3.9: Calculation procedure for determining the required $n_f t_f$

3.7 Verification of proposed model

3.7.1 Analytical verification

A non-linear analysis model of a reinforced concrete column presented in Chapter 5 was developed based on an existing model proposed by Matrin (2007). In the model, a column was divided into two parts includes elastic and plastic parts. A discretion section method was applied to plastic part so that a section was slice into independent fibers, each concrete fiber was modeled as a non-linear spring, and each reinforcing was presented by an assembly of three non-linear springs including: steel spring, lap splice spring, and embed spring. An effectiveness of FRP was taken into account by updating these non-linear springs, for example: a confined effect (presented in section 2.2.1) is applied into confined concrete springs' properties; a proposed model (presented in this chapter) was applied to calculate lap splice strength, and then incorporated in analytical model by updating lap splice springs' characteristics.

The developed model was applied to simulate some existing experiments. The verifications of both predicted lap splice strength and column's dynamic behavior were presented in section 5.2. It is noted that, ether rectangular section column or circular section column were verified.

3.7.2 Experimental verification

A proposed tri-uniform bond stress distribution model was used for designing 16 columns (in beam's tested-setting) with four series of lap splice length. A proposed procedure to obtain a required number of FRP (presented in section 3.6) was used to calculate the number of FRP sheets wrapped in experiment. A static load was applied to determine a beam strength, a lap splice strength and a bond stress distribution as well.

An experimental design, testing and result are shown in section 4.1, 4.3 and 4.4; the experimental verification of lap splice strength and proposed bond stress distribution is analyzed and presented in section 4.4.5.

3.8 Parametric investigation

The proposed tri-uniform bond stress model for predicting the strength of lap splice confined by FRP are examined as per parametric study to investigate the effect of influencing parameters, such as the ratio of lap splice length to bar diameter L_s/d_b, the ratio of concrete cover to bar diameter c/d_b, the amount of transverse reinforcements and the number and thickness of FRP layers. The hypothetical column section is 200mm wide $\times$ 400mm deep as shown in Fig 3.10. The section is reinforced longitudinally by $8\phi 14$ (deformed bar with 14 mm diameter) and transversely by $\phi 8$ spaced at 200 mm. The yield strength f_y of bars is 550 MPa and the elastic modulus E_s is 1.96 x 10^5 MPa. The unconfined concrete compressive strength $f_c'$is 39 MPa. The FRP sheet is 0.13 mm thick and the elastic modulus E_f is 2.30 x 10^5 MPa.

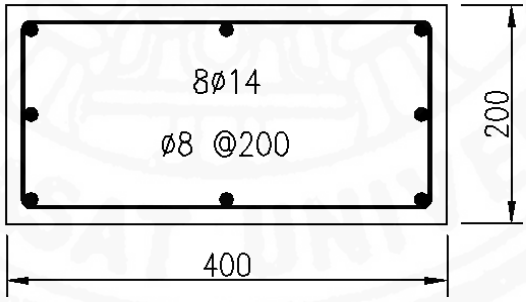

Fig 3.10: Column section used in parametrical investigation

3.8.1 Strength of lap splice length Ls = 20db, 25db, 30db and 35db

The ratio of concrete cover to bar diameter c/d_b varies from 1.0 to 2.4. For each value of c/d_b, the number of FRP sheets is changed in order to assess the effect of FRP thickness on the strength of lap splice. Fig 3.11 to Fig 3.14 show the relationship between lap splice strength and the number of FRP sheets for four selected values of L_s/d_b. As can be observed in Fig 3.11 to Fig 3.14, for the columns confined by the same amount of FRP, the lap splice strength is higher in the columns with larger concrete cover. It is also found that the rate of strength increase with respect to the number of FRP layers is faster in the pre-yield range than in the post-yield range. This would be expected because the bond strength

in the yielding zone is normally smaller than the elastic zone. In pre-yield range, the strength increase varies linearly with the number of FRP layers. In post-yield range, the strength increases in a nonlinear decreasing rate owing to the yielding in the bars. These figures are useful for design because the number of FRP layers to develop a required strength for a given lap splice length and ratio of concrete cover to bar diameter can be obtained. It should be noted that the developed lap splice strength predicted by the model is associated with the splitting failure mode only. In reality, the bar may fracture before reaching the post-yield splitting strength and the actual strength of the bar is therefore governed by the yielding strength.

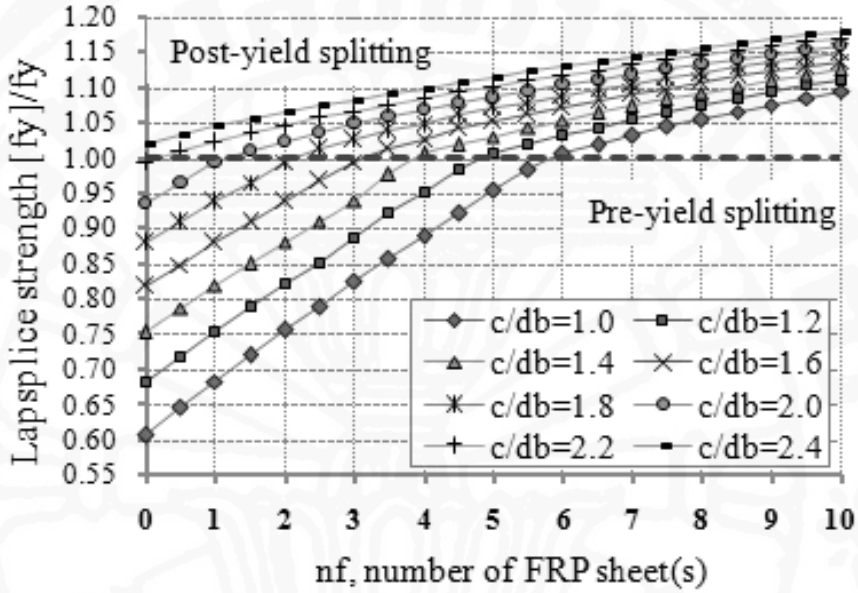

Fig 3.11: Strength of lap splice $L_s/d_b = 20$

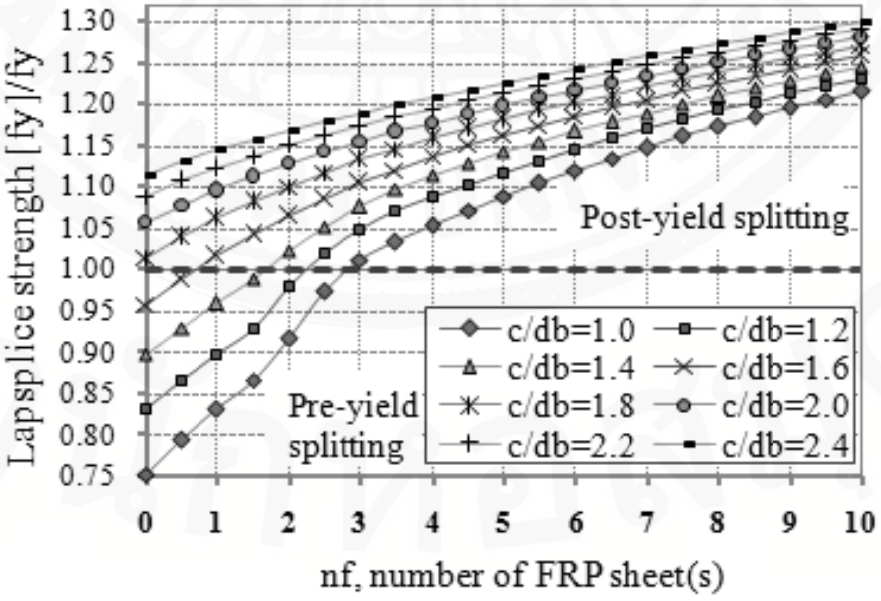

Fig 3.12: Strength of lap splice ($L_s/d_b = 25$)

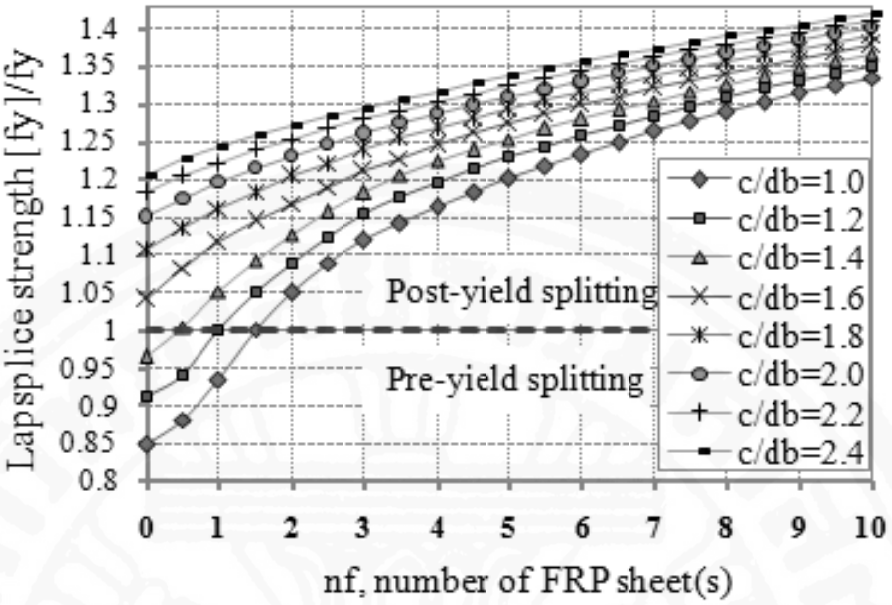

Fig 3.13: Strength of lap splice ($L_s/d_b = 30$)

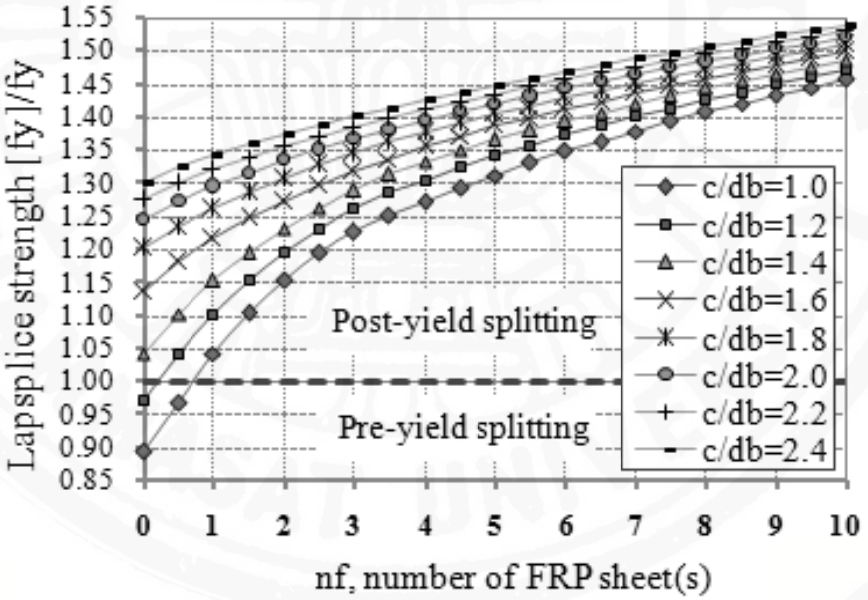

Fig 3.14: Strength of lap splice ($L_s/d_b = 35$)

3.8.2 Required number of FRP sheets to develop the a specified lap splice strength

Fig 3.15 shows a relationship between a required number of FRP sheets and lap spliced length (L_s) in order to develop the lap splice strength of $1.25f_y$. Here the factor 1.25 is selected to ensure an adequate excess of strength over the bar nominal yield strength. In the graph, eight values of ratio of concrete cover to bar diameter c/d_b are plotted versus the lap splice length of $20d_b$, $25d_b$, $30d_b$ and $35d_b$. As can be seen, the required number of

FRP sheets reduces as the lap splice length increases. At the same lap splice length, the required number of FRP layers is reduced as the ratio of concrete cover to bar diameter increases. As can be seen from the graph, the nonlinear relation between the required FRP layers versus lap splice length is evident. For instance, at $c/d_b = 1.6$, the increase in L_s/d_b from 20 to 30 (1.5 times) results in the decrease in the required number of FRP layers from 20 to 5 (about 4 times). The reduction rate is faster for the short lap splice length. It can also be seen that for any values of L_s/d_b, increasing the lap splice length by $5d_b$ can decrease the number of FRP layers by two times. This shows a high impact of lap splice length to bar diameter ratio on the required number of FRP layers. This prediction seems to qualitatively agree with Bousias's experimental results (Bousias, Spathis et al. (2006)). Bousias tested a series of columns with variable lengths of lap splice 15, 30, 45 d_b and with two and five layers of FRP sheets in each column. They found that FRP significantly increased the strength of lap splice when the length of lap splice was relatively short, say $15d_b$, but did not show a marked capacity improvement in case of longer lap splice (30-45d_b).

This implies that the required FRP sheets are highly sensitive to lap splice length when lap splice length is relatively short and not so in case of a longer lap spice length.

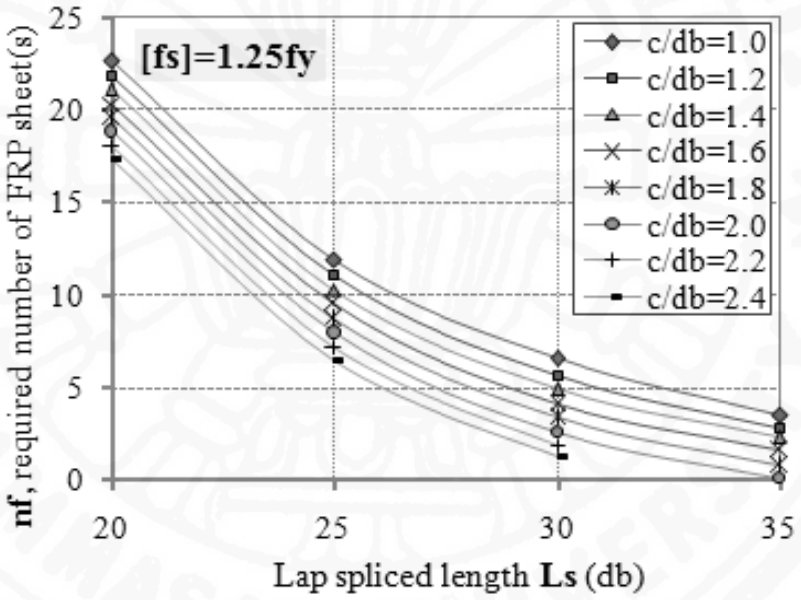

Fig 3.15: Required FRP sheets versus lap spliced length

Fig 3.16 shows the relationship between the required number of FRP sheets to develop 1.25f_y strength and ratio of concrete cover to bar diameter for four selected values of L_s/d_b. Basically, the data in Fig 3.16 are the same as those in Fig 3.15. It can be seen that the required number of FRP layers decreases linearly with the increase in c/d_b. This is rooted in Eq. (3.2) in which the terms c/d_b and $n_f t_f$ both appear as linear terms inside the parenthesis. Thus, when c/d_b changes linearly, the $n_f t_f$ must also change linearly in an inverse manner to keep the same bond strength u_{sp}. Physically, the terms $n_f t_f$ and c/d_b both refer to the same confining effect. Thus, when the confinement provided by concrete or c/d_b increases, the required confinement from FRP is proportionally decreased.

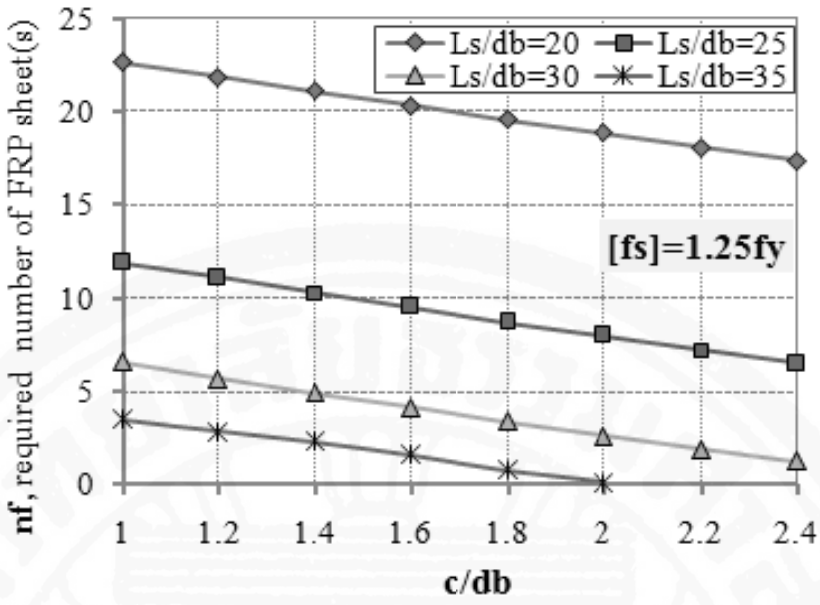

Fig 3.16: Required FRP sheets versus c/d_b